

## Angular dependence of positive exchange biasing in GdFe/FeMn bilayers

J. Du<sup>a)</sup>

National Laboratory of Solid State Microstructures, Nanjing University, Nanjing 210093, People's Republic of China

D. Z. Yang

Surface Physics Laboratory (National Key Laboratory) and Department of Physics, Fudan University, Shanghai 200433, People's Republic of China

X. J. Bai, X. S. Wu, and A. Hu

National Laboratory of Solid State Microstructures, Nanjing University, Nanjing 210093, People's Republic of China

S. M. Zhou

Surface Physics Laboratory (National Key Laboratory) and Department of Physics, Fudan University, Shanghai 200433, People's Republic of China

L. Sun

Department of Mechanical Engineering, University of Houston, Houston, Texas 77204

(Presented on 3 November 2005; published online 17 April 2006)

For Gd<sub>45</sub>Fe<sub>55</sub>/Fe<sub>50</sub>Mn<sub>50</sub> bilayers, both negative and positive exchange biasing have been observed for low and high magnetic cooling field  $H_{CF}$ , respectively. These results can be attributed to a competition between antiferromagnetic coupling at GdFe/FeMn interface and the Zeeman energy of FeMn spins under  $H_{CF}$ . In order to reveal the magnetization reversal mechanism, the angular dependence of  $H_E$  and  $H_C$  has been investigated. It is found that the negative exchange biasing and the positive one have similar angular dependence that can be described by a magnetization coherent rotation model. © 2006 American Institute of Physics. [DOI: 10.1063/1.2151803]

### I. INTRODUCTION

Exchange biasing (EB) in ferromagnet(FM)/antiferromagnet (AFM) bilayers has been extensively studied in the past decade because of its crucial importance in magneto-electronic devices. While the common negative EB can be observed in a variety of FM/AFM bilayers, positive EB has been mainly limited to fluoride-based FM/AFM bilayers as well as rare-earth (RE) transition (TM)-based systems.<sup>1-5</sup> For fluoride-based FM/AFM bilayers, the positive EB is attributed to the competition of the Zeeman energy of the AFM spins in the external magnetic field and the antiferromagnetic coupling at the FM/AFM interface.<sup>1</sup> Superexchange coupling between FM and AFM layers has been thought to be the major reason for the antiferromagnetic coupling at the interface in fluoride-based FM/AFM bilayers.<sup>6</sup> Although the exchange interaction between TM and RE spins is argued to be responsible for the antiferromagnetic coupling in GdFe/NiCoO bilayers, superexchange coupling cannot be rigorously excluded.<sup>7</sup>

The mechanism of the magnetization reversal in FM/AFM bilayers with the positive EB remains unclear because the coherent rotation model and spiral spin structure in AFM layers both can explain the experimental results. Since the angular dependence of magnetization reversal is strongly related to EB mechanism, the measurement of positive exchange biasing at different orientations and the comparison to negative exchange biasing are very important to unravel the nature of the positive EB. So far, only very limited

studies of positive EB have been performed.<sup>8,9</sup> In this work, GdFe(=Gd<sub>45</sub>Fe<sub>55</sub>)(15 nm)/FeMn(=Fe<sub>50</sub>Mn<sub>50</sub>)(10 nm) bilayers were fabricated by magnetron sputtering, in which no superexchange coupling can exist. As the magnetic cooling field  $H_{CF}$  is increased, the exchange field  $H_E$  changes from negative values to positive ones. Apparently, antiferromagnetic coupling between the FM and AFM magnetizations should exist. Studies of the angular dependence of  $H_E$  and  $H_C$  were performed, indicating that the magnetization reversal is based on coherent rotation in the current system.

### II. EXPERIMENTS

A large specimen of GdFe(15 nm)/FeMn(10 nm) bilayer was deposited on Si(100) at ambient temperature by magnetron sputtering. The base pressure was  $2 \times 10^{-5}$  Pa and an Ar pressure of 0.33 Pa was maintained during deposition. GdFe and FeMn layers were made by dc sputtering from a GdFe composite target and an FeMn alloy target, respectively. To form a GdFe composite target, small Gd pieces were placed on the Fe sputtering target. Before deposition of bilayer, a 30 nm thick Cu buffer layer was prepared to stimulate the sequent growth of the FeMn layer with fcc (111) preferred orientation. Finally, another 30 nm thick Cu layer was used to avoid oxidation. The deposition rates of GdFe, FeMn, and Cu layers were 0.3, 0.1, and 0.2 in units of nm/s, respectively. During deposition, a magnetic field of about 130 Oe was applied parallel to the film plane to induce an in-plane uniaxial anisotropy in the FM layer. The compositions of GdFe and FeMn were analyzed by x-ray fluorescence spectroscopy. Magnetic hysteresis (MH) loops at low temperatures were measured by a commercial physical prop-

<sup>a)</sup>Author to whom correspondence should be addressed; electronic mail: jdu@nju.edu.cn

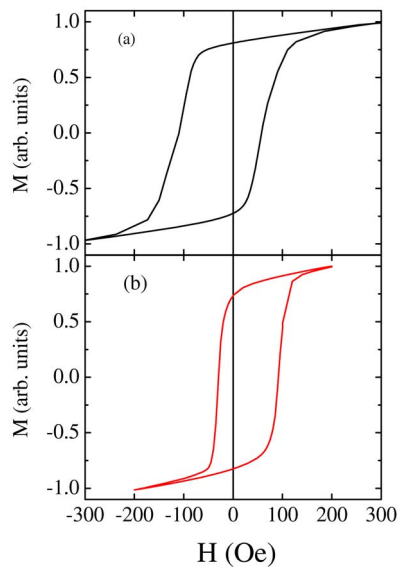


FIG. 1. (Color online) Typical in-plane hysteresis loops of GdFe/FeMn bilayer at 5 K, with  $H_{CF}=300$  Oe (a) and 60 kOe (b). The external magnetic field is parallel to the cooling field.

erty measurement system (PPMS). The sample was heated to 400 K and cooled to 5 K under an external magnetic field, i.e., the cooling field, and MH loops were then measured during warmup. Magnetization loops at various orientations were measured at room temperature by a vibrating sampling magnetometer (VSM) from Lakeshore Company.

### III. RESULTS AND DISCUSSION

Figure 1 shows typical hysteresis loops of the GdFe/FeMn bilayer at 5 K, after field cooling under 60 kOe and 300 Oe external field parallel to the film plane. It clearly shows that  $H_E$  is positive for  $H_{CF}=60$  kOe and negative for  $H_{CF}=300$  Oe. Detailed studies of the dependence of  $H_E$  and  $H_C$  on  $H_{CF}$  were also carried out and the behaviors were very similar to that of GdFe/NiCoO bilayers as we reported before,<sup>7</sup> which can be summarized in the following. With increasing  $H_{CF}$ ,  $H_E$  changes sharply from negative to positive at small  $H_{CF}$  and finally approaches saturation. At the critical value  $H_{CF}^0$  for the crossover,  $H_E$  is equal to zero.  $H_C$  increases sharply with initial increasing  $H_{CF}$  and reaches a maximum at  $H_{CF}^0$ . After that,  $H_C$  decreases as  $H_{CF}$  is further increased. In experiments, we found that at  $H_{CF}=60$  kOe,  $H_E$  and  $H_C$  increase as the GdFe thickness decreases, which is due to the interfacial nature of the EB in GdFe/FeMn bilayers.

The sign change of the  $H_E$  with  $H_{CF}$  can be easily understood as follows. First, the physical reason for the antiferromagnetic coupling between the FeMn and GdFe layers is addressed as follows. Since the AFM layer presented here is simply composed of Fe and Mn atoms, the superexchange coupling can be rigorously excluded, which is argued to exist in fluoride-based FM/AFM bilayers. There are negative exchange interactions between Gd-Mn, Gd-Fe, and Mn-Fe atoms (Fe atoms exist in both layers), and positive exchange interactions between Fe-Fe atoms in GdFe and FeMn layers as well. Since the magnetic moment of the Gd sublattice is

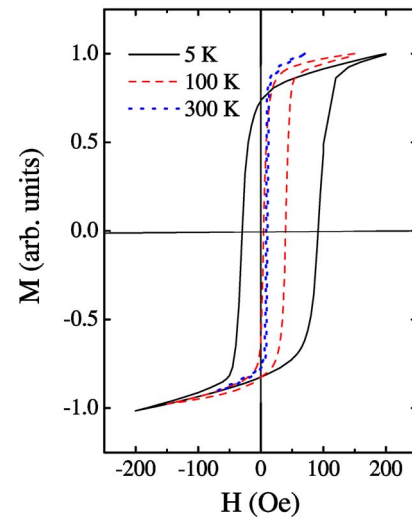


FIG. 2. (Color online) Typical in-plane hysteresis loops of GdFe/FeMn bilayer at 5 K (solid line), 100 K (dash line), and 300 K (dotted line), respectively, where the cooling field  $H_{CF}=60$  kOe. The measurement magnetic field is parallel to the cooling field.

larger than that of the Fe sublattice for the  $Gd_{45}Fe_{55}$  alloys, it is quite reasonable to conclude that GdFe and FeMn layers are coupled antiferromagnetically. Second, the sign change of the exchange field with  $H_{CF}$  in Fig. 1 can be explained as a result of the competition between antiferromagnetic coupling energy of FM and AFM spins and the Zeeman energy of the AFM spins under the external magnetic field  $H_{CF}$ .  $H_E$  changes to positive values if  $H_{CF}$  is large enough to align the FeMn interface magnetization along  $H_{CF}$ , thus overcoming the interface antiferromagnetic coupling between GdFe and FeMn layers. On the contrary, for small  $H_{CF}$ ,  $H_E$  maintains negative values. Therefore, similar to the explanations for fluoride- or NiCoO-based FM/AFM bilayers,<sup>1,7</sup> the sign change of the exchange field with  $H_{CF}$  can be explained.

The variations of  $H_E$  and  $H_C$  with temperature can be clearly observed in Fig. 2. For  $H_{CF}=60$  kOe,  $H_E$  and  $H_C$  decrease monotonically with increasing temperature. At 5, 100, and 300 K, the  $H_E$  is 61, 31, and 10 Oe, and the  $H_C$  is 1, 17.5, and 31 Oe, respectively. With the data of  $H_E$ ,  $M_{FM}$ , and  $t_{FM}$ , the exchange coupling energy ( $\Delta\sigma=H_E M_{FM} t_{FM}$ ) can be calculated. It is 0.0033 erg/cm<sup>2</sup> at room temperature, which is much smaller than that of FeNi/FeMn bilayers. This might be due to the amorphous structure of the GdFe layer. It is very interesting to find that for high cooling fields (like  $H_{CF}=60$  kOe)  $H_E$  always remains positive in the entire measuring temperature range. This is because in this case the Zeeman energy can overcome the antiferromagnetic coupling in the whole measuring temperature region, although the interfacial exchange coupling energy is enhanced at low temperature. The decrease of  $H_E$  and  $H_C$  with increasing temperature is due to a reduction of the anisotropic energy of the AFM layers or of the interfacial exchange coupling energy at high temperatures, depending on the mechanism of the EB. One can also find that for the GdFe/FeMn bilayer the reduction of the exchange field with increasing temperature coincides with a linear scale of the exchange field in FeMn-based bilayers with temperature.<sup>10</sup> If the magnitude of the cooling field is very small, the Zeeman energy may not overcome the

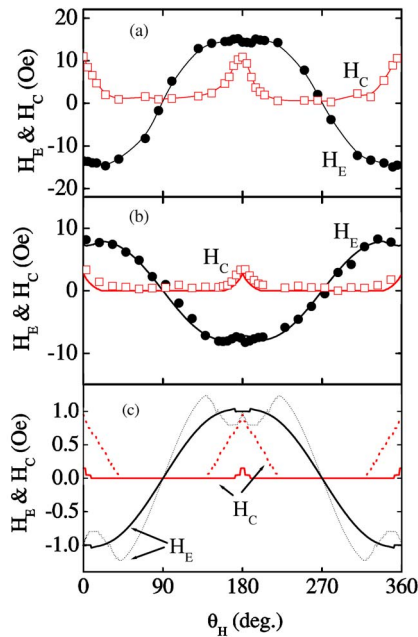


FIG. 3. (Color online) Angular dependence of  $H_E$  and  $H_C$  obtained for  $H_{CF}=300$  Oe (a) and 60 kOe (b), where the temperature is 300 K. The solid lines refer to the calculated results. In (c) the angular dependence of normalized  $H_E$  and  $H_C$  was calculated with  $H_C/H_E=0.2$  (solid lines) and 1.0 (dotted lines).

AFM coupling at any temperature, and  $H_E$  will remain negative at all temperatures. At an intermediate cooling field,  $H_E$  may have a crossover from negative to positive with the variation of temperature. All the above phenomena have been clearly observed in GdFe/NiCoO bilayers.<sup>7</sup>

It is instructive to compare the angular dependence of the positive EB with that of the negative one for an identical sample since it is strongly related to the characteristic of the samples, such as the exchange coupling energy, the domain wall energy of the AFM layers, and so on. Figure 3 shows the angular dependence of the negative EB in Fig. 3(a) and the positive one in Fig. 3(b) for the GdFe/FeMn bilayer, where  $H_{CF}=300$  Oe and 60 kOe, respectively. Here,  $\theta_H$  is the angle between the measuring magnetic field and the cooling field. For measurements,  $H_E$  exhibits the unidirectional symmetry, i.e.,  $H_E(\theta_H)=H_E(-\theta_H)=-H_E(180\pm\theta_H)$ , whereas  $H_C$  shows the uniaxial symmetry, i.e.,  $H_C(\theta_H)=H_C(-\theta_H)=H_C(180\pm\theta_H)$ . Remarkably, the negative EB and the positive one have almost the same angular dependence, indicating the same magnetization reversal mechanism. In the vicinity of  $\theta_H=0$  and 180 deg,  $H_E$  in the two cases has a small valley. Apparently, the angular dependence of the  $H_E$  cannot be described by a simple cosine function of  $\theta_H$  and high order terms must be considered.<sup>11</sup> Our calculations in Fig. 3(c) indicate that the small valley is induced by the uniaxial anisotropy in the GdFe layer. The valley depth is determined by the ratio of the coercivity and the exchange field at  $\theta_H=0$  and increases with the increase of the ratio. The coercivity decreases sharply to zero when the external magnetic field is deviated from  $\theta_H=0$  and 180 deg. Similar phenomena were also found in other bilayer systems and were attributed to the fact that the magnitude of the uniaxial anisotropic field

is much smaller than the unidirectional anisotropic field, and the easy axis of the AFM grains is strictly aligned along the cooling field.<sup>12-15</sup> Finally, a coherent rotation model has been employed to calculate the angular dependence of the positive and negative EB in order to further reveal the magnetization reversal mechanism.<sup>16</sup> As shown in Fig. 3, the calculated results (the solid lines) are in good consistency with the experimental results. This indicates that, although the spin structure near the interface may be modified to some extent for the positive EB, the magnetization reversal mechanism can still be approximately considered within the framework of coherent rotation model.

#### IV. CONCLUSIONS

In summary, the exchange biasing effect and its angular dependence for GdFe/FeMn bilayers have been systemically investigated. With the cooling field increasing,  $H_E$  shows a crossover from negative to positive values. This results from antiferromagnetic coupling between GdFe and FeMn layers, where the superexchange coupling is unambiguously absent. Simulation based on a coherent rotation model can be adopted to explain well the angular dependence of both positive and negative exchange biasing in GdFe/FeMn bilayers. The similarity between the positive and negative EB also suggests that the same magnetization reversal mechanism in the exchange biased GdFe/FeMn bilayers.

#### ACKNOWLEDGMENTS

This work was supported by the National Natural Science Foundation of China Grant Nos. 10174014, 62071013, 10021001, 10321003, and 60490290, and the State Key Project of Fundamental Research Grant Nos. 2001CB610602 and 2002CB613504, and Shanghai Nanotechnology Program Center (No. 0252nm004).

- <sup>1</sup>J. Nogués, D. Lederman, T. J. Moran, and I. K. Schuller, Phys. Rev. Lett. **76**, 4624 (1996).
- <sup>2</sup>C. Leighton, J. Nogués, B. J. Jönsson-Åkerman, and I. K. Schuller, Phys. Rev. Lett. **84**, 3466 (2000).
- <sup>3</sup>S. Mangin, F. Montaigne, and A. Schuhl, Phys. Rev. B **68**, 140404 (2003).
- <sup>4</sup>F. Canet, C. Bellouard, S. Mangin, C. Chatelain, C. Senet, R. Siebrecht, V. Leiner, and M. Piecuch, Eur. Phys. J. B **34**, 381 (2003).
- <sup>5</sup>S. Demirtas, A. R. Koymen, and H. Zeng, J. Phys.: Condens. Matter **16**, L213 (2004).
- <sup>6</sup>T. M. Hong, Phys. Rev. B **58**, 97 (1998).
- <sup>7</sup>D. Z. Yang, J. Du, L. Sun, X. S. Wu, X. X. Zhang, and S. M. Zhou, Phys. Rev. B **71**, 144417 (2005).
- <sup>8</sup>I. N. Krivorotov, C. Leighton, J. Nogus, I. K. Schuller, and E. D. Dahlberg, Phys. Rev. B **68**, 054430 (2003).
- <sup>9</sup>M. J. Pechar, D. Bennett, Nienchtze Teng, C. Leighton, J. Nogus, and I. K. Schuller, Phys. Rev. B **65**, 064410 (2002).
- <sup>10</sup>See, e.g., J. Nogués and I. K. Schuller, J. Magn. Magn. Mater. **192**, 203 (1999).
- <sup>11</sup>T. Ambrose, R. L. Sommer, and C. L. Chien, Phys. Rev. B **56**, 83 (1997).
- <sup>12</sup>L. E. Fernandez-Outon and K. O'Grady, J. Magn. Magn. Mater. **290-291**, 536 (2005).
- <sup>13</sup>T. Mewes, H. Nembach, M. Rickart, S. O. Demokritov, J. Fassbender, and B. Hillebrands, Phys. Rev. B **65**, 224423 (2002).
- <sup>14</sup>J. Geshev, L. G. Pereira, and J. E. Schmidt, Phys. Rev. B **66**, 134432 (2002).
- <sup>15</sup>J. Camarero, J. Sort, A. Hoffmann, J. Miguel García-Martín, B. Dieny, R. Miranda, and J. Nogués, Phys. Rev. Lett. **95**, 057204 (2005).
- <sup>16</sup>H. W. Xi, M. H. Kryder, and R. M. White, Appl. Phys. Lett. **74**, 2687 (1999).